LATTICE BOLTZMANN SIMULATION OF MAGNETHYDRODYNAMICS NATURAL CONVECTION FLOW FOR SALT WATER IN A HORIZONTAL CYLINDRICAL ANNULUS[*]

H. R. ASHORYNEJAD, K. SEDIGHI, M. FARHADI[**] AND E. FATTAHI

Faculty of Mechanical Engineering, Babol University of Technology, Babol, I. R. of Iran
Email: mfarhadi@nit.ac.ir

Abstract– Natural convection of an electrically conducting fluid under the different directions of magnetic field in a horizontal cylindrical annulus is numerically studied using lattice Boltzmann method (LBM). The inner and outer cylinders are maintained at uniform temperatures. Detailed numerical results of heat transfer rate, temperature and velocity fields have been presented for salt water with Pr=13.2, Ra=10^5 to 10^6 and Ha=0 to 100 for three directions of magnetic field. The computational results reveal that in horizontal cylindrical annulus the flow and heat transfer are suppressed more effectively by direction and intensity of magnetic field. It is also found that the flow oscillations can be suppressed effectively by imposing an external horizontal magnetic field. The average Nusselt number increases with rise in radius ratio but decreases with the Hartmann number. Furthermore, it can be observed that there is a good agreement between the present result and those predicted by available benchmark solutions under the limiting conditions.

Keywords– Hartman number, cylindrical annulus, magnetic field, lattice Boltzmann method

1. INTRODUCTION

Magnetic fluid can be limited, positioned, shaped, and controlled by magnetic fields. Using these interesting characteristics, many practical studies have been carried out [1-4], such as, sealing devices, levitation, actuator, and inertia damper. The other applications of magnetic field are crystal growth processes. It is an established physical fact that the motion of an electrically conducting fluid is suppressed by the presence of a magnetic field and considerable experimental evidence supports this conclusion. Gotoh and Yamada [5] studied thermal convection in a horizontal layer of magnetic fluid known as the Benard problem. These investigators obtained the connection between the critical Rayleigh number and the magnetization of boundaries by the Galerkin method. Schwab and Stierstadt [6, 7] examined the problem experimentally. Natural convection of magnetic fluid, which is called thermomagnetic convection, is different from that of a Newtonian fluid for the reason that a magnetic body force exists in addition to gravitational and buoyant forces. Therefore, it is estimated that convection of a magnetic fluid can be controlled by varying an applied magnetic field. Bashtovoy et al [8] examined the effect of the magnetic field on convective heat transfer in a cavity at the square cross-section. Berkovsky et al [9] conducted a numerical and experimental study of laminar heat convection in a vertical circular magnetic fluid layer on a cylindrical energized cable. Alchaar et al. [10] presented an analytical solution for the study of natural convection in a rectangular two-dimensional shallow cavity under the influence of an external magnetic field. The influence of magnetic field on free convection in a cavity was studied by Rudraiah et al. [11]. They found that the effect of magnetic field is to reduce the rate of heat transfer.

Sellers and Walker [12] have studied the steady liquid-metal flow through a rectangular duct with electrically insulated walls in the presence of variable magnetic field. Several studies have also been carried out to examine the effects of magnetic field on Czochralski crystal growth and other phase change problems in the cavity. Most of the studies found in the literature on the consequence of magnetic field on free convection are mainly confined to rectangular enclosures. Little attention has been given to the study of free convection of electrically conducting fluids in a cylindrical annulus in the presence of a magnetic field though its important applications. To understand the right effects of an applied magnetic field and to perform a correct analysis of flow mechanism, it is important to understand its effect for a wide range of physical and geometrical parameters. Such a study helps in understanding the effective control of convection by the applied magnetic field which has some application in crystal growth problems. The LBM is a new method for simulating fluid flow and modeling physics of fluids [13-15]. Various numerical simulations have been performed using different thermal LB models or Boltzmann-based schemes to investigate the natural convection problems [16-18]. This method has also been successfully applied to flow with MHD flow [19]. In general, these lattice Boltzmann MHD models fall into two categories: the multi-speed (MS) approach and multi-distribution-function (MDF) approach. The MS approach is an uncomplicated extension of the lattice Boltzmann models [20, 21] in which a tensor (i.e., two-indexed) particle representation and a bi-directional streaming mechanism are used. For each one of these particles, there are two vectors attached, representing the momentum and magnetic fields. These MS models introduce some additional discrete velocities and the equilibrium distributions usually include higher order velocity terms. However, this model is confined to low-Reynolds number because the values of the transport coefficients at the stability threshold are finite and its extension to three dimension would require a large amount of computational memory. Such limitations severely restrict the MDF model's applications [22]. However, the limitations of the MS approach can be partly overcome by the MDF approach. In the MDF model presented by Dellar [23], the Lorentz force can be introduced as a point-wise force, the induction equation is also solved using an LBGK equation by introducing an independent distribution function. MDF models can improve the numerical stability. The accuracy of the MDF models has been verified by several benchmark studies [19, 24]. Despite the benefit of the MDF models, there are still some limitations. For instance, in order to get the correct macroscopic equation from the MDF models, it must be assumed that the Mach number of the flow is small and the density varies. This model was used for simulating the effect of magnetic field on natural convection in porous cavity and nanofluid in the cavity too [25, 26].

In the present study, natural convection of magnetic fluid in concentric annuli made of two isothermal horizontal cylinders was investigated using the Lattice Boltzmann method. Effect of Ha number and angle of magnetic force on heat transfer and flow field was investigated.

2. THE LATTICE BOLTZMANN METHOD

In the following, $\mathbf{e}_\alpha$ will denote the discrete velocity set, where α is between 0 and 8.

$$\mathbf{e}_\alpha = \begin{cases} (0,0) & \alpha = 0 \\ (\cos[(\alpha-1)\pi/4], \sin[(\alpha-1)\pi/4])c & \alpha = 1,2,3,4 \\ \sqrt{2}(\cos[(\alpha-1)\pi/4], \sin[(\alpha-1)\pi/4])c & \alpha = 5,6,7,8 \end{cases} \qquad (1)$$

Where $c = \dfrac{\Delta x}{\Delta t}$, Δx and Δt are the lattice cell size and the lattice time step size, respectively.

For simplicity, in lattice Boltzmann method $\Delta x = \Delta t = 1$ is assumed. But in this work the magnetic space discretization is the D2Q5 model. In the following, $\mathbf{e}_\beta$ will denote the discrete magnetic set, where β is between 0 and 4.

$$\mathbf{e}_\beta = \begin{cases} (0,0) & \beta = 0 \\ (\cos[(\beta-1)\pi/4], \sin[(\beta-1)\pi/4])c & \beta = 1,2,3,4 \end{cases} \tag{2}$$

For incompressible flow the lattice Boltzmann equations of velocity, temperature and magnetic field can be given respectively by:

$$g_\alpha(\mathbf{x}+e_\alpha\Delta t, t+\Delta t) - g_\alpha(\mathbf{x},t) = -\frac{1}{\tau_T}\left[g_\alpha(\mathbf{x},t) - g_\alpha^{eq}(\mathbf{x},t)\right] \tag{3}$$

$$f_\alpha(\mathbf{x}+e_\alpha\Delta t, t+\Delta t) - f_\alpha(\mathbf{x},t) = -\frac{1}{\tau_m}\left[f_\alpha(\mathbf{x},t) - f_\alpha^{eq}(\mathbf{x},t)\right] + \Delta t\, e_\alpha F_k \tag{4}$$

$$h_\beta(\mathbf{x}+e_\beta\Delta t, t+\Delta t) - h_\beta(\mathbf{x},t) = -\frac{1}{\tau_b}\left[h_\beta(\mathbf{x},t) - h_\beta^{eq}(\mathbf{x},t)\right] \tag{5}$$

Where f_α^{eq}, g_α^{eq} and h_α^{eq} are the equilibrium distribution functions for velocity, temperature and magnetic field which are expressed as:

$$f_\alpha^{eq} = w_\alpha(1+\frac{3}{c^2}\mathbf{e}_\alpha\mathbf{u}+\frac{9}{2c^4}(\mathbf{e}_\alpha\mathbf{u})^2 - \frac{3}{2c^2}\mathbf{u}\mathbf{u}) + \frac{9w_\alpha}{2c^4}(\frac{1}{2}|\mathbf{B}|^2|\mathbf{e}_\alpha|^2 - (\mathbf{e}_\alpha\mathbf{B})^2) \tag{6}$$

$$g_\alpha^{eq} = w_\alpha T(1+\frac{3}{c^2}\mathbf{e}_\alpha\mathbf{u}) \tag{7}$$

$$h_\beta^{eq} = \Omega_\beta(\mathbf{B}+3\mathbf{e}_\beta(\mathbf{uB}-\mathbf{Bu})) \tag{8}$$

Where:

$$w_\alpha = \begin{cases} 4/9 & \alpha = 0 \\ 1/9 & \alpha = 1,2,3,4 \\ 1/36 & \alpha = 5,6,7,8 \end{cases} \qquad \Omega_\beta = \begin{cases} 1/3 & \beta = 0 \\ 1/6 & \beta = 1,2,3,4 \end{cases} \tag{9}$$

w_α and Ω_β are the equilibrium distribution weight for direction α and β.
F_k is the external force in the direction of lattice velocity, which in order to incorporate buoyancy force in the model, the force term in the Eq. (3) needs to be calculated as shown below in vertical direction (y):

$$F_k = 3w_\alpha g_y \beta\theta \tag{10}$$

The Boussinesq approximation was applied and radiation heat transfer is negligible; τ is the relaxation time which can be given by:

$$v = c_s^2(\tau_m - \frac{1}{2}) \qquad \alpha = c_s^2(\tau_T - \frac{1}{2}) \qquad \eta = c_s^2(\tau_b - \frac{1}{2}) \tag{11}$$

Where ν, α and η are the kinematical viscosity, diffusivity coefficient and the magnetic resistivity

respectively and $c_s = \dfrac{c}{\sqrt{3}}$ the speed of sound.

The macroscopic variables were obtained for distribution functions as follows:

$$\rho = \sum_{\alpha} f_{\alpha}, \quad \rho\mathbf{u} = \sum_{\alpha} \mathbf{e}_{\alpha} f_{\alpha}, \quad T = \sum_{\alpha} g_{\alpha}, \quad \mathbf{B} = \sum_{\beta} h_{\beta} \tag{12}$$

Finally, Eq. (3), Eq. (4) and Eq. (5) are usually solved in two steps:

Collision step

$$\tilde{f}_{\alpha}(\mathbf{x}, t+\Delta t) = -\frac{1}{\tau_m}\Big[f_{\alpha}(\mathbf{x},t) - f_{\alpha}^{eq}(\mathbf{x},t) \Big] - f_{\alpha}(\mathbf{x},t) \tag{13.1}$$

$$\tilde{g}_{\alpha}(\mathbf{x}, t+\Delta t) = -\frac{1}{\tau_T}\Big[g_{\alpha}(\mathbf{x},t) - g_{\alpha}^{eq}(\mathbf{x},t) \Big] - g_{\alpha}(\mathbf{x},t) \tag{13.2}$$

$$\tilde{h}_{\beta}(\mathbf{x}, t+\Delta t) = -\frac{1}{\tau_b}\Big[h_{\beta}(\mathbf{x},t) - h_{\beta}^{eq}(\mathbf{x},t) \Big] - h_{\beta}(\mathbf{x},t) \tag{13.3}$$

Streaming step

$$f_{\alpha}(\mathbf{x}+e_{\alpha}\Delta t, t+\Delta t) = \tilde{f}_{\alpha}(\mathbf{x}, t+\Delta t) \tag{14.1}$$

$$g_{\alpha}(\mathbf{x}+e_{\alpha}\Delta t, t+\Delta t) = \tilde{g}_{\alpha}(\mathbf{x}, t+\Delta t) \tag{14.2}$$

$$h_{\beta}(\mathbf{x}+e_{\beta}\Delta t, t+\Delta t) = \tilde{h}_{\beta}(\mathbf{x}, t+\Delta t) \tag{14.3}$$

Where $\tilde{f}_{\alpha}, \tilde{g}_{\alpha}, \tilde{h}_{\beta}$ denotes the post-collision distribution function. Eq.13 is the so called collision step.

a) Curved boundary treatment

Figure 1 shows a part of an arbitrary curved wall geometry separating a solid region from fluid where the black small circles on the boundary x_w, the open circles represent the boundary nodes in the fluid region x_f and the grey solid circles indicate those in the solid region x_b. In the boundary condition $\tilde{f}(\mathbf{x}_b,t), \tilde{g}(\mathbf{x}_b,t), \tilde{h}(\mathbf{x}_b,t)$ are needed to perform the streaming steps on fluid nodes $\mathbf{x}_f$. The fraction of an intersected link in the fluid region Δ is defined by:

$$\Delta = \frac{\left\| \mathbf{x}_f - \mathbf{x}_w \right\|}{\left\| \mathbf{x}_f - \mathbf{x}_b \right\|} \tag{15}$$

For treating velocity and temperature field in curved boundaries the method reported in [27-30] is used. For the magnetic field, the methods are based on an extrapolation method of second-order accuracy applied in [31]. The Chapman–Enskog expansion for the post-collision distribution function on the Eq. (13c) is used as [31]:

$$\tilde{h}_{\bar{\beta}}(\mathbf{x}_b, t+\Delta t) = (1-\chi_m)\tilde{h}_{\beta}(\mathbf{x}_f, t+\Delta t) + \chi_m h_{\beta}^{o}(\mathbf{x}_b, t+\Delta t) - 6\Omega_{\beta}\mathbf{e}_{\alpha} \cdot \Lambda_w^{o}$$
$$+\Omega_{\beta}\zeta_m[(\mathbf{B}_w - \mathbf{B}_f) - s(\mathbf{B}_{bf} - \mathbf{B}_f)] \tag{16}$$

Where:

$$h_\beta^o(\mathbf{x}_b, t + \Delta t) = \Omega_\beta [\mathbf{B}_{bf} + 3e_\beta \Lambda_{bf}^o], \quad \Lambda^o = \mathbf{uB} - \mathbf{Bu} \tag{17}$$

$$\mathbf{B}_{bf} = \mathbf{B}_{ff}, \ \Lambda_{bf}^o = \Lambda_{ff}^o, \ \zeta_m = \frac{\tau_b + (1-\chi_m)(\tau_b - 1) - \chi_m}{\Delta - s}, \chi_m = \frac{2\Delta - 1}{\tau_b - 2} \Bigg\} \ \ if \ \ 0 < \Delta < \frac{1}{2} \tag{18}$$

$$\begin{aligned} \mathbf{B}_{bf} = (1 - \frac{1}{\Delta})\mathbf{B}_f + \frac{1}{\Delta}\mathbf{B}_w, \ \Lambda_{bf}^o = (1 - \frac{1}{\Delta})\Lambda_f^o + \frac{1}{\Delta}\Lambda_w^o, \\ \zeta_m = \frac{\tau_b + (1-\chi_m)(\tau_b - 1) - \chi_m}{\Delta + s}, \ \chi_m = \frac{2\Delta - 1}{\tau_b} \end{aligned} \Bigg\} \ \ if \ \ \frac{1}{2} \le \Delta \le 1 \tag{19}$$

$\mathbf{B}_w$ denotes the magnetic of solid wall, $\mathbf{B}_{bf}$ is the imaginary magnetic for interpolations and $\mathbf{e}_{\bar{\beta}} \equiv -\mathbf{e}_\beta$.

3. COMPUTATIONAL DOMAIN AND NUMERICAL DETAILS

The physical model used in this work is shown in Fig. 2. A two dimensional horizontal annulus with an inner radius R_i and an outer radius R_o is used and φ is measured counterclockwise from the upward horizontal plane through the center of cylinders. The inner and outer cylinder surfaces are maintained at different uniform temperatures T_i and T_o respectively, where $T_i > T_o$ is assumed. The magnetic field is applied on the cylinders with specific direction. The working fluid which is salt water has Pr = 13.2. The Rayleigh number (Ra), and Hartmann number (Ha) for the current problem are defined as follows:

$$Ra = g b \mathrm{D} T (R_o - R_i)^3 / a u \qquad\qquad Ha = B(R_o - R_i)/\sqrt{\upsilon\eta} \tag{20}$$

Local, average and mean Nusselt numbers are defined on wall cylinder as *Nu, Nu_{avr} and Nu_{mean}* :

$$Nu = R_i \ln\left(\frac{R_o}{R_i}\right)\frac{\partial T}{\partial r}\bigg|_{r = R_i} \qquad Nu_{avr} = \frac{1}{pR}\int_0^p (Nu)r\,dj \qquad Nu_{mean} = \frac{Nu_{avr}\big|_{R_i} + Nu_{avr}\big|_{R_o}}{2} \tag{21}$$
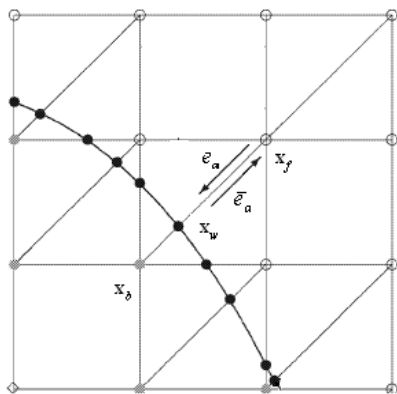
Fig. 1. Layout of the regularly spaced lattices and curved wall boundary
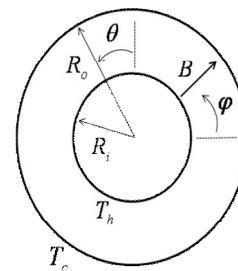
Fig. 2. Geometry of problems

4. RESULTS AND DISCUSSIONS

In this study the steady, axisymmetric, magnetohydrodynamic (MHD) flow of a viscous, Newtonian, incompressible, electrically-conducting fluid through an isotropic between two concentric cylinders in the presence of a oriented magnetic field is assumed. Numerical computations in the present study were carried out for salt water with *Pr=13.2* . The effect of static magnetic field on the buoyancy-driven convection of an electrically conducting fluid in a horizontal cylindrical annulus is investigated by LBM

approach. To validate the numerical simulation, both the local and the mean equivalent thermal conductivity were obtained at different Rayleigh numbers for a natural convection in concentric horizontal annulus. Results have been compared with the study of Kuehn and Goldstein [32]. An equivalent thermal conductivity, K_{eq} was used to compare the accuracy of the present computations. The average equivalent heat conductivity was defined for the inner and outer cylinders by:

$$\overline{K}_{eqi} = -\frac{\ln(rr)}{\pi(rr-1)}\int_0^\pi \frac{\partial T}{\partial r}d\varphi \qquad\qquad \overline{K}_{eqo} = -\frac{rr\ln(rr)}{\pi(rr-1)}\int_0^\pi \frac{\partial T}{\partial r}d\varphi \qquad (22)$$

This parameter was defined as the actual heat flux divided by the heat flux that would occur by pure conduction in the absence of magnetic field. The computed average equivalent heat conductivity for the case of Pr=0.71 and λ=2.6 was compared with the previous study [32]. Results of local equivalent thermal conductivity were shown in Fig. 3a and it represented good agreement with the experiments of Kuhen and Goldstein [32]. In Table 1, computed mean equivalent thermal conductivity was compared with the results of Kuhen and Goldstein [33] in which three Ra numbers were considered.

(a)   (b)
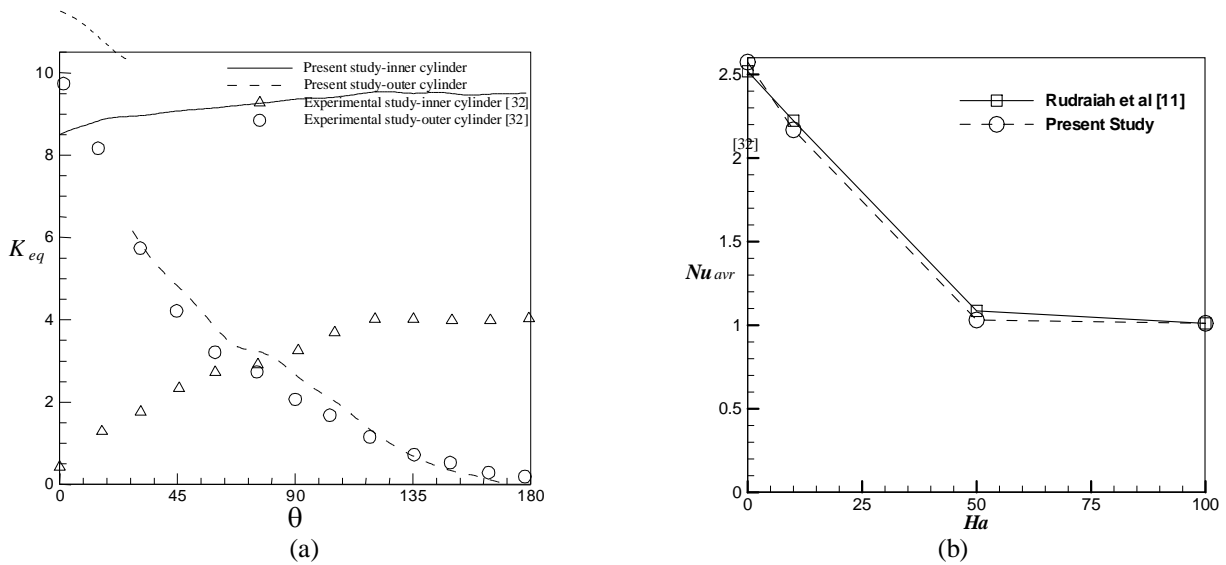
Fig. 3. Comparison between this study and previous work at (a) equivalent thermal conductivity at Ra=5*10^4(b) average Nusselt number at $Gr = 2\times10^4$ under various Hartmann number

Table 1. Mean equivalent thermal conductivity at Pr=0.7compared with the results of Kuehn and Goldstein [33]

	Ra=1.31×10^3	Ra=1.29×10^4	Ra=1.02×10^5
Kuehn and Goldstein [33]	1.14	2.25	3.66
present study	1.14	2.22	3.53

To validate the effect of magnetic field on the natural convection the simulation was performed for the analysis of natural convection in a rectangular cavity with magnetic field; the results were compared with those reported by Rudraiah *et al* [11] in Fig. 3b. They numerically investigated the effect of a transverse magnetic field on natural-convection flow inside a rectangular enclosure at Grashof number = 2×10^4.

These effects provide credence to the accuracies of the present numerical solutions. Uniform grid was employed in the present study.

To test and assess grid independence of the solution scheme, numerical experiments were performed as shown in Table 2. Different mesh combinations were used for the case of $Ra = 5\times10^5$, $Ha = 50$ and for salt water. The present code was tested for grid independence by calculating the average Nusselt number on the cylindrical walls. It was found that a grid size of 120×120 ensures the grid independent solution for this case.

Table 2. Comparison of the mean Nusselt number (Nu_{mean}) for different grid resolution
at $Ra = 5 \times 10^5$, $Ha = 50$ and $\lambda = 2$

Mesh size	*80×80*	*100×100*	*120×120*	*140×140*	*160×160*
Nu_{mean}	*1.2170*	*1.2612*	*1.3212*	*1.3359*	*1.3319*

The convergence criterion for the termination of all computations is:

$$\max_{grid} \left| \Gamma^{n+1} - \Gamma^n \right| \leq 10^{-7} \qquad (23)$$

Where n is the iteration number and Γ stands for the independent variables like temperature or velocity. The buoyancy force is naturally more effective for higher Rayleigh numbers. The Lorentz force, which reduces velocities and suppresses the convection, will be stronger with increasing Hartmann number. The effects of intensity and direction of magnetic field on isotherms between the cylinders were shown in Fig. 4. Pattern of isotherms was affected strongly by changing the intensity and direction of the magnetic field. There is a high temperature gradient at the bottom of the cylinder in the absence of magnetic field. With increasing the Raleigh number this temperature gradient increases. At the specified area where magnetic field is perpendicular on the isothermal walls the Lorentz force resists the Buoyancy force. Consequently a large vortex is divided to a small vortex at this area. Thus natural convection is damped by increasing Ha number in this area, which can be due to the weaker intensity of the small vortex. The effects of intensity and direction of magnetic field on stream lines between the cylinders were shown in Fig. 5. As can be observed in the presence of vertical magnetic field, small vortexes were created at the top and bottom of the cylinders, whereas in the presence of the horizontal magnetic field the broken vortexes shift along the direction of the magnetic field. The isotherms become parallel and the temperature gradient decreases at this region. Also, horizontally applied magnetic field caused parallel isotherms at the wide region of the created bottom cylinder. It should be mentioned that there are some increased temperature gradients at the small area on the top side of the inner cylinder.
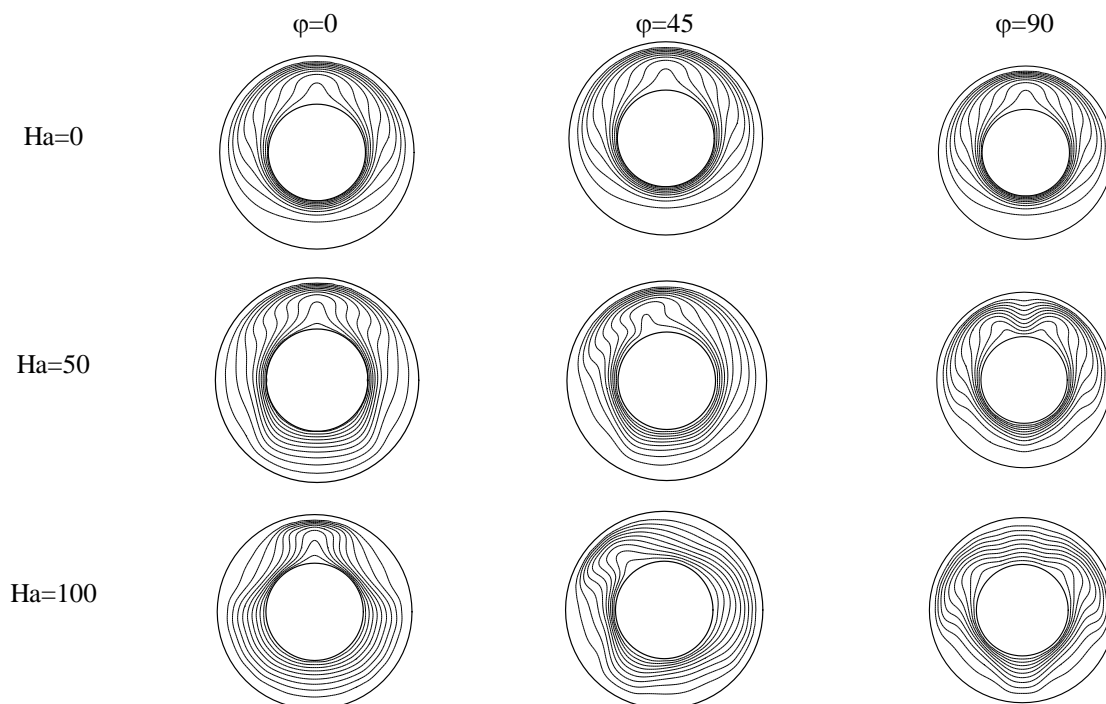
Fig. 4. Effect of transverse magnetic field on the isotherm lines with variable
angle at the Ra=5×105 , with the λ=2
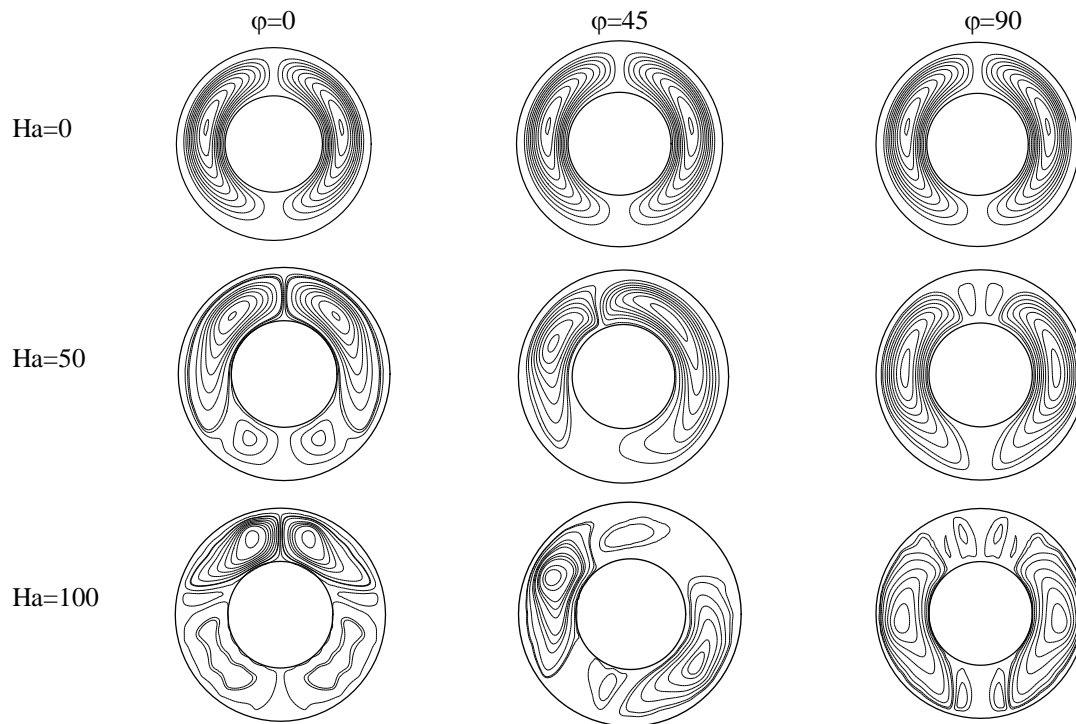
Fig. 5. Effect of transverse magnetic field on the stream lines with variable
angle at the Ra=5×10^5 , with the λ=2

The effect of magnetic field on isotherms at different Ra numbers was shown in Fig. 6. It can be seen that the horizontal magnetic field involves the Lorenz force in the opposite direction of the buoyancy force, consequently the convective heat transfer became weaker and conduction heat transfer became dominant at the bottom of the inner cylinder. Also, the isotherms become concentric and parallel between the cylinders at this region, especially at low Ra number. However, by increasing the Ra number, the buoyancy force will become stronger; therefore, conduction heat transfer becomes dominant at the higher Ha number. The results depicted that for Ra=10^5, the isotherms become parallel at Ha=50 and for Ra=5×10^5 and Ra=10^6 this occurs for lower half cylinders at Ha=75 and Ha=100 respectively.

Mean Nusselt number was sharply increased by the increase of Rayleigh number at low Ha. This effect was reduced by the increase of the magnetic field (Fig. 7a). Minimum mean Nusselt number occurred almost at the Ha=100 in different Rayleigh number at the present horizontal magnetic field. The effect of different angle of magnetic field on average Nusselt number with Ra=5×10^5 was shown in Fig. 7b.

It is also found that, increase in Ha number in the vertical direction caused a decrease in the temperature gradient on the top and bottom of the cylinder and consequently a maximum drop of the mean Nusselt number occurred at higher Ha number in the vertical direction, as can be observed in Fig. 7b.

The radius ratio varied between 2 and 4. An increase in the gap width, i.e., an increase in λ, increased the temperature gradient on the inner cylinder at lower Ha number. As can be inferred from Fig. 8a, increasing the radius ratio raises the mean Nusselt number, whereas with increasing intensity of the magnetic field the mean Nusselt number sharply falls. This is the same trend as for vertical magnetic fields, although the value of mean Nusselt number in this case is a little less than for the horizontal magnetic fields. Mean Nusselt number continuously decreased by increasing Ha at the different radius ratio at the vertical magnetic field, while minimum mean Nusselt number appeared at Ha=100 and λ=2 for φ=90 as can be seen in Fig. 8b.
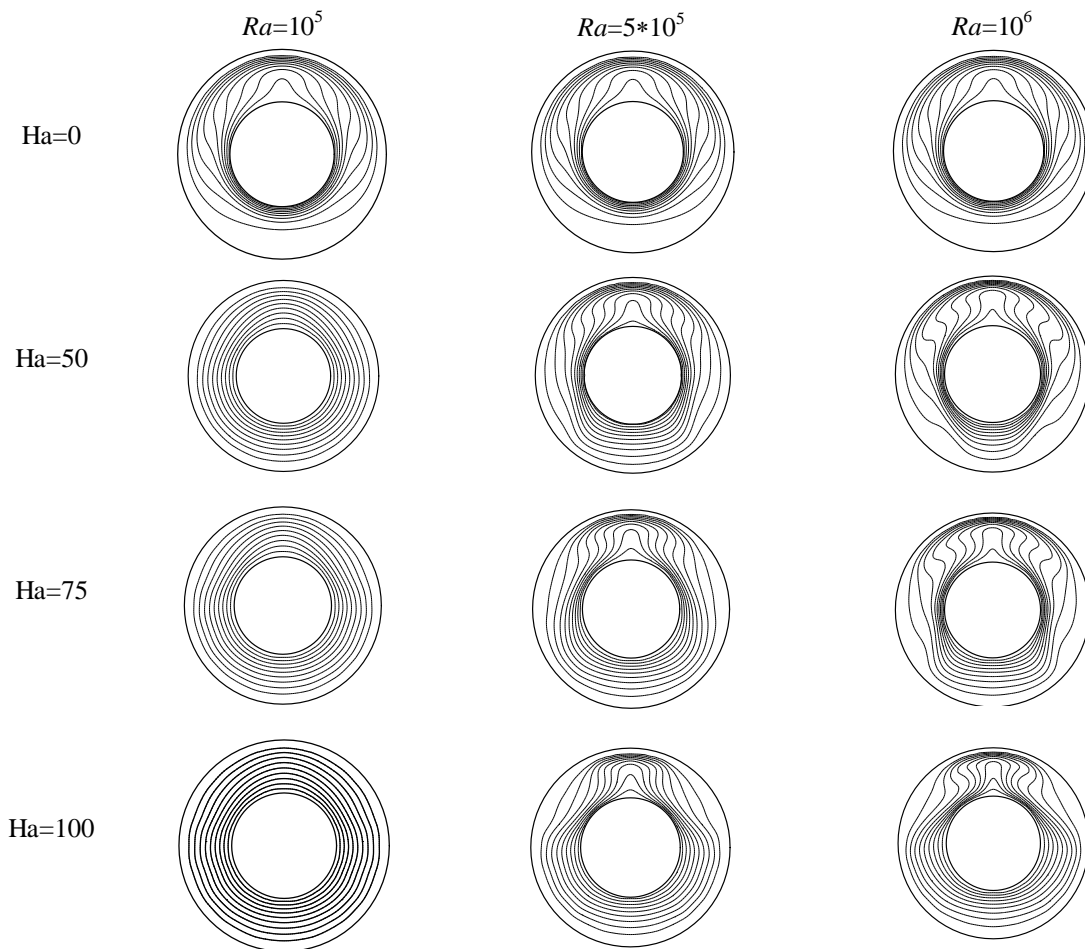
Fig. 6. Effect of horizontal magnetic field on the isotherms lines at the variables Rayleigh number with λ=2

(a)

(b)
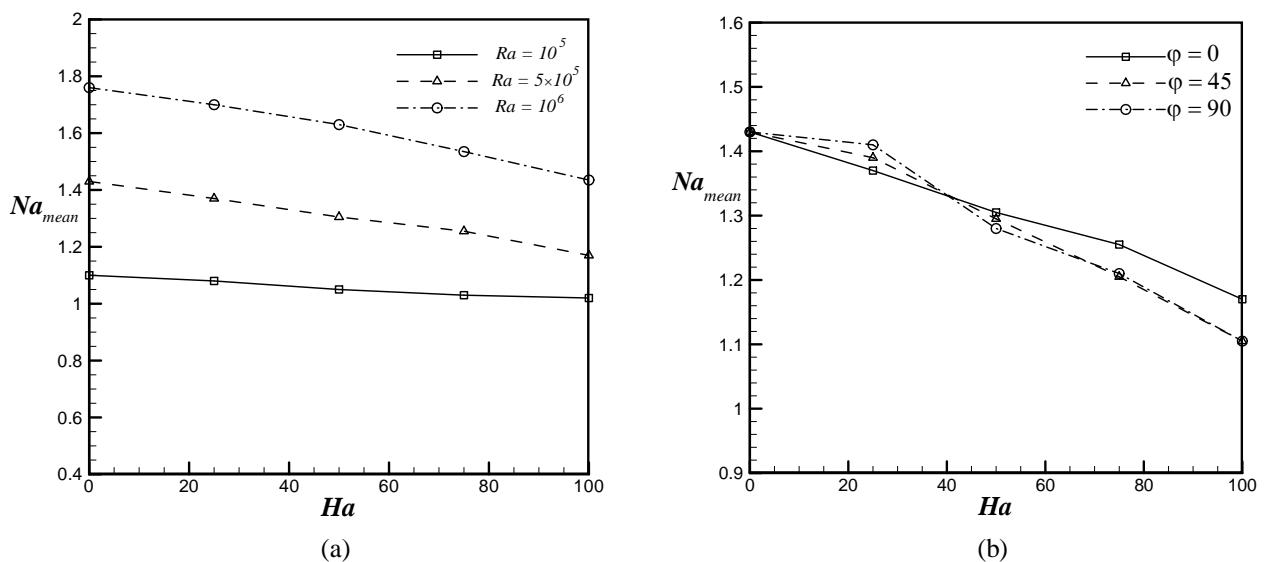
Fig. 7. Effect of Rayleigh number and direction of magnetic field on the mean Nusselt number with λ=2, (a) φ=0, (b) Ra=5×10⁵
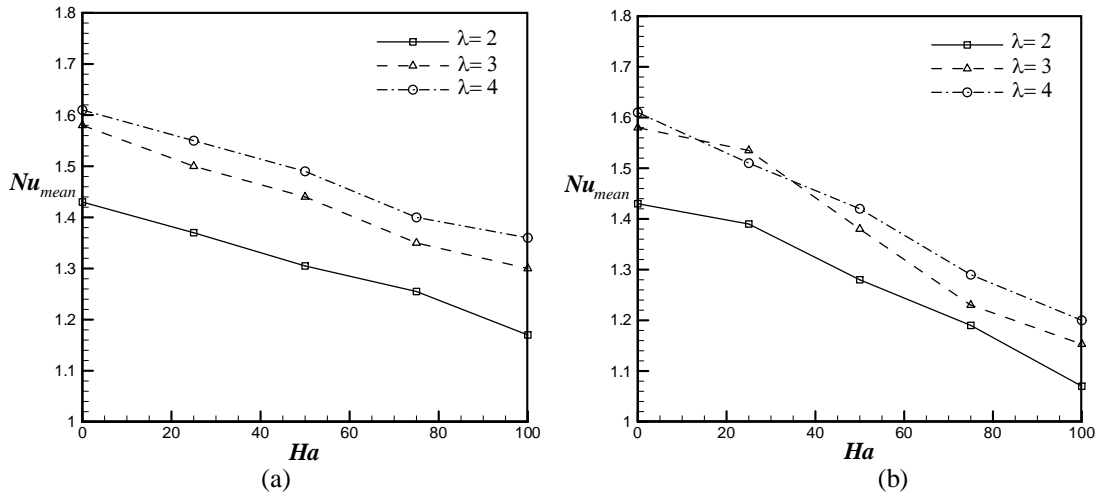
Figure 8. Effect of magnetic field and radius ratio on the mean Nusselt number with
Ra=5×10^5, a) φ=0 , b) φ=90

5. CONCLUSION

Natural convection flow in horizontal annulus enclosure in the presence of magnetic field was simulated numerically. The Lattice Boltzmann method based on multi-distribution function was used for modeling flow, thermal and magnetic fields. The computational results reveal that the flow and heat transfer were more effectively suppressed by the direction and intensity of the magnetic field. This study shows that Lattice Boltzmann method based on multi-distribution function is a powerful approach for simulating MHD natural convection in the geometry that include curved boundaries. Results show that mean Nusselt number is sharply increased by the increase in Rayleigh number at low Ha. This effect is reduced by an increase in the Ha number. The increment of radius ratio can increase mean Nusselt number, although the effect is less significant compared to the Rayleigh number. On closer inspection, it is noted that at the specified area where magnetic field is perpendicular on the isothermal walls the Lorentz force resists the Buoyancy force. Consequently the large vortex is divided into a small vortex at this area. Minimum mean Nu number occurrs at higher Ha number when the applied magnetic field is vertical.

NOMENCLATURE

e_α	=	Discrete lattice velocity in direction
c_s	=	Speed of sound in Lattice scale
B	=	magnetic flux density (T)
Ha	=	Hartmann number $(B(R_o - R_i)/\sqrt{\upsilon\eta})$
f_k^{eq}	=	Equilibrium distribution
g_y	=	Acceleration due to gravity, (ms^{-2})
k	=	Thermal conductivity $(W/m.K)$
r	=	radial coordinate
Pr	=	Prandtl number (ν/α)
Nu_{avr}	=	Average Nusselt number
Nu	=	Local Nusselt number along surfaces
R_i, R_o	=	radius of the inner and outer cylinders
R	=	Dimensionless radius $(r - R_i)/(R_o - R_i)$

F_{ext}	=	External force
T_h	=	Hot temperature (K)
T_c	=	Cold temperature (K)

Greek symbols

α	=	Thermal diffusivity (m^2/s)
υ	=	Kinematic viscosity (m^2/s)
η	=	Magnetic resistivity (m^2/s)
θ	=	tangential direction
φ	=	magnetic field angle
ρ	=	Density (kg/m^3)
τ	=	Lattice relaxation time
Δt	=	Lattice time step
λ	=	radius ratio, (R_o/R_i)

REFERENCES

1. Al Omari, S.A.B., Haik, Y. & Abu Jdayil, B. (2010). Flow characteristics of gallium in a meso-scale channel under the influence of magnetic fields. *Int. Communications in Heat and Mass Transfer 37*, pp. 1127–1134.

2. Ibáñez, G. & Cuevas, S. (2010). Entropy generation minimization of a MHD (magnetohydrodynamic) flow in a micro channel. *Energy*, Vol. 35, pp. 4149-4155.

3. Kandasamy, R., Hashim, I., Kamis, A. B. & Muhaimin, I. Combined heat and mass transfer in MHD free convection from a wedge with ohmic heating and viscous dissipation in the presence of suction and injection. *Iranian Journal of Science & Technology, Transaction A*, Vol. 31, pp. 151-162.

4. Osalusi, E., Side, J. & Harris, R. (2008). Thermal-diffusion and diffusion-thermo effects on combined heat and mass transfer of a steady MHD convective and slip flow due to a rotating disk with viscous dissipation and Ohmic heating, Int. *Communications in Heat and Mass Transfer*, Vol. 35, pp. 908–915.

5. Gotoh, K. & Yamada, M. (1982). Thermal convection in a horizontal layer of magnetic fluids. *J. Phys. Soc. Jpn.*, Vol. 5, pp. 13042-3048.

6. Schwab, L. & Stierstadt, K. (1987). Field-induced wave vector-selection by magnetic benard-convection. *J. Magn. Magn. Mat*., Vol. 65, pp. 315-316.

7. Schwab, L. (1990). Thermal convection in ferrofluids under a free surface. *J. of Magnetism and Magnetic Materials*, Vol. 85, pp. 199-202.

8. Bashtovoy, V. G., Isayev, S.V., Pavlinov, M. P., Polevikov, V. K. & Ye, V. (1978). Fertman, thermal convection in a ferromagnetic fluid in an inhomogeneous magnetic field. *Heat Transfer Soviet Res.*, Vol. 1, No. 05-9.

9. Berkovsky, B. M., Fertman, V. E., Poleviktov, V. K. & Isaev, S. V. (1978). Specific *Features of Natural Convection Heat Transfer in Magnetic Fluids. 6th International Heat Transfer Conference*, Toronto, Canada, 147-151.

10. Alchaar, S., Vasseur, P. & Bilgen, E. (1995). Natural convection in a rectangular enclosure with a transverse magnetic field, Trans. *ASME J. Heat Transfer*, Vol. 11, p. 7668–673.

11. Rudraiah, N., Barron, R. M., Venkatachalappa, M. & Subbaraya, C. K. (1995). Effect of a magnetic field on free convection in a rectangular enclosures. *Int. J. Eng. Sci.*, Vol. 33, pp. 1075–1084.

12. Sellers, C. C. & Walker, J. S. (1999). Liquid-metal flow in an electrically insulated rectangular duct with a non-uniform magnetic field. *Int. J. Eng. Sci.*, Vol. 37, pp. 541–552.

13. Nemati, H., Sedighi, K., Farhadi, M., Pirouz, M. M. & Fattahi, E. (2010). Numerical simulation of fluid flow of two rotating side-by-side circular cylinders by Lattice Boltzmann method. *Int. J. Computational Fluid Dynamics*, Vol. 2, pp. 83–94.

14. Delavar, M. A., Farhadi, M. & Sedighi, K. (2010). Numerical simulation of direct methanol fuel cells using lattice Boltzmann method. *Int. J. Hydrogen Energy*, Vol. 35, pp. 9306-9317.

15. Delavar, M. A., Farhadi, M. & Sedighi, K. (2009). Effect of the heater location on heat transfer and entropy generation in the cavity using the Lattice Boltzmann method. *Heat Transfer Research*, Vol. 40, pp. 521–536.

16. Rabienataj Darzi, A. A., Farhadi, M., Sedighi, K., Fattahi, E. & Nemati, H. (2011). Mixed convection simulation of inclined lid driven cavity using lattice Boltzmann method. *Iranian Journal of Science and Technology Transaction B*, Vol. 35, pp. 209-219.

17. Dixit, H. N., Babu, V. (2006). Simulations of high Rayleigh number natural convection in a square cavity using the lattice Boltzmann method, Int. J. Heat Mass Transfer 49, 727–739, (2006).

18. Mishra, S. C., Mondal, B., Kush, T. & Siva Rama Krishna, B. Solving transient heat conduction problems on uniform and non-uniform lattices using the lattice Boltzmann method. *Int. Communications in Heat and Mass Transfer*, Vol. 36, pp. 322–328.

19. Dellar, P. J. (2002). Lattice kinetic schemes for magnetohydrodynamics. *J. Comp. Phys.*, Vol. 179, pp. 95-126.

20. Feng, M. C., Chang, S. B. & Wang, C. X. (2005). Lattice bhatnagar gross krook simulations in 2-D incompressible magnetohydrodynamics. *Commun. Theor. Phys.*, Vol. 44, pp. 917–920.

21. MacNab, A., Vahala, G., Pavlo, P., Vahala, L. & Soe, M. (2001). Lattice boltzmann model for dissipative incompressible MHD. *Fusion and Plasma Phys*, Vol. 25A, pp. 853-856.

22. Wang, C. X. & Chang, S. B. (2005). A new lattice Boltzmann model for incompressible magneto hydrodynamics incompressible. *Chinese Physics*, Vol. 14.

23. Dellar, P. J. (2009). Moment equations for magnetohydrodynamics. *J. Stat. Mech.*, P06003.

24. He, X., Chen, S. & Doolen, G. D. (1998). A novel thermal model for the lattice Boltzmann method in incompressible limit. *J. Comp. Phys.*, Vol. 146, pp. 282-300.

25. Hasanpour, A., Farhadi, M., Sedighi, K. & Ashorynejad, H. R. (2010). Lattice boltzmann simulation for magneto hydrodynamic flow in a mixed convective flow in a porous medium. *World applied sciences J.*, Vol. 11, No. 9, 1124–1132.

26. Nemati, H., Farhadi, M., Sedighi, K., Ashorynejad, H. R. & Fattahi, E. (2012). Magnetic field effects on natural convection flow of nanofluid in a rectangular cavity using the Lattice Boltzmann model. *Scientia Iranica*, Vol. 19, pp. 303-310.

27. Guo, Z. L., Zheng, Ch. & Shi, B. C. (2002). An extrapolation method for boundary conditions in lattice Boltzmann method. *Phys. Fluids.*, Vol. 14, pp. 2007–2010.

28. Mei, R., Yu, D., Shyy, W., Luo, L. Sh. (2002). Force evaluation in the lattice Boltzmann method involving curved geometry. *Phys. Rev.*, Vol. E 65, pp. 1–14.

29. Fattahi, E., Farhadi, M. & Sedighi, K. (2010). Lattice Boltzmann simulation of natural convection heat transfer in eccentric annulus. *Int. J. Thermal Sciences*, Vol. 49, pp. 2353-2362.

30. Yu, D., Mei, R., Luo, L. S. & Shyy, W. (2003). Viscous flow computations with the method of lattice Boltzmann equation. *Progr. Aerospace Sci.*, Vol. 39, pp. 329–367.

31. Pattison, M. J., Premnath, K. N., Morley, N. B. & Abdou, M. A. (2008). Progress in lattice Boltzmann methods for magnetohydrodynamic flows relevant to fusion applications. *Fusion Engineering and Design*, Vol. 83, pp. 557–572.

32. Kuehn, T. & Goldstein, R. (1976). An experimental and theoretical study of natural convection in the annulus between horizontal concentric cylinders. *J. Fluid Mech.*, Vol. 74, pp. 695–719.

33. Kuehn, T. & Goldstein, R. (1978). An experimental study of natural convection heat transfer in concentric and eccentric horizontal cylindrical annuli. *J. Heat Transfer*, Vol. 100, pp. 635–40.